

LIQUID FILM IN MICRO TUBE TWO PHASE FLOW SYSTEMS

Naoki Shikazono*, Youngbae Han, Hiroshi Kanno and Gyeonghwan Lee

Institute of Industrial Science, The University of Tokyo, 4-6-1 Komaba, Meguro-ku, Tokyo 153-8505, Japan.

*E-mail: shika@iis.u-tokyo.ac.jp

ABSTRACT

The thickness of liquid film formed between confined vapour bubble and tube wall in micro tubes is one of the most important parameters which dominate two phase flow heat transfer in micro tubes. In the present work, laser confocal method is applied to measure liquid film thickness. It is investigated that liquid film thickness under steady condition depends basically on capillary number, but it also shows strong dependence on Reynolds number even in laminar flow regime. Under flow boiling or condensation conditions, bubble velocity is not constant but accelerated or decelerated due to phase change. The importance of flow acceleration and deceleration on the formation of liquid film is investigated. Finally, simple scaling analyses are conducted to obtain predictive correlations for the initial liquid film thickness.

KEYWORDS: Micro two phase flow, Liquid film thickness, Laser confocal method,

1. INTRODUCTION

Two phase flow in micro-scale is one of the emerging topics in energy researches. For example, the efficiency of compact boilers for waste heat recovery steam engines [1], water flooding tolerances of porous gas diffusion layer in Polymer Electrolyte Fuel Cell electrodes [2] strongly depend on micro two phase flow characteristics. However, micro-scale two phase flows are very different from macroscopic flows, and thus designing two-phase flow systems still remains as a difficult task. One of the major flow regimes in micro scale is the slug flow. Liquid film formed between confined vapour bubble and tube wall in micro tubes or channels plays an important role in heat transfer, since local heat conduction is effectively enhanced at the thin liquid film region. It is reported that the liquid film thickness is one of the most important parameters for predicting two phase flow heat transfer in micro tubes [3].

Many researches have been conducted to investigate the characteristics of liquid film both experimentally and theoretically. Taylor [4] was the pioneer to measure liquid film thickness in a slug flow. Aussillous & Quere [5] experimentally reinvestigated liquid film thickness and found that the thickness deviates from Taylor's data at high Reynolds numbers. Kreutzer et al. [6] studied liquid film thickness and pressure drop in a micro tube both numerically and experimentally. Predicted liquid film thickness also showed Reynolds number dependence even in laminar flow range.

Recently, experimental techniques for measuring micro two phase flows have shown great progress, e.g. optical interface detection, laser extinction, light reflection and laser confocal displacement, etc [7]. These methods are expected to contribute a lot for collecting precise information of micro two phase flows.

However, at the moment, quantitative data for local and instantaneous liquid film thicknesses are still limited. In order to develop heat transfer models for micro-scale two phase flows, it is crucial to know liquid film thickness accurately. In the present study, liquid film thicknesses measurement studies using laser confocal method by the authors are summarized [8-12]. Series of systematic experiments is conducted to investigate the effects of parameters such as viscous, surface tension and inertial forces, cross sectional shapes and flow acceleration. In addition, simple scaling analyses are conducted to obtain predictive correlations for the initial liquid film thickness.

2. EXPERIMENTAL PROCEDURES

In this section, experimental setup and procedures are described. Refer to the original papers by the authors for details [8-11]. Figure 1 shows the schematic diagram of the experimental setup. Circular tubes made of Pyrex glass with inner diameters of $D_h \approx 0.3, 0.5, 0.7, 1.0$ and 1.3 mm, square quartz tubes with $D_h \approx 0.3, 0.5$ and 1.0 mm, and high aspect ratio rectangular quartz channels with $D_h \approx 0.2, 0.6$ and 1.0 mm were used. Table 1 show the dimensions of the tested tubes. One side of the tube was connected to the syringe and the actuator motor (EZHC6A-101, Oriental motor), which were used to control the liquid velocity in the test section. The velocity of the gas-liquid interface was measured from the images captured by the high speed camera (Phantom 7.1, Photron SA1.1). Laser confocal displacement meter (LT9010M, Keyence) was used to measure the liquid film thickness. The resolution for the present laser confocal displacement meter is $0.01 \mu\text{m}$, the laser spot diameter is $2 \mu\text{m}$ and the response time is $640 \mu\text{s}$. Horizontal flow condition is applied throughout the experiment. Liquid film thickness initially decreases and

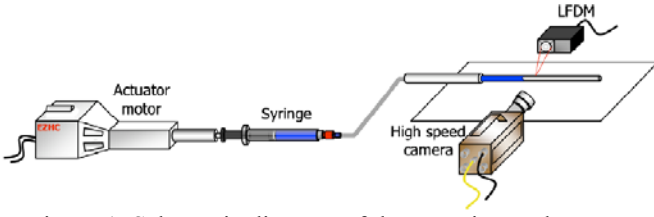


Figure 1 Schematic diagram of the experimental setup.

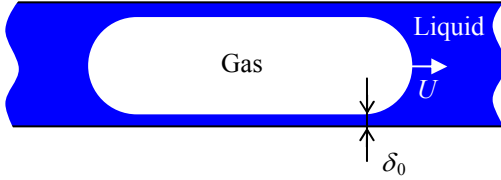


Figure 2 Initial liquid film thickness δ_0 .

Table 1 Dimensions of the tested tubes.

	Hydraulic diameter D_h [mm]	H [mm]	W [mm]	Aspect ratio
Circular tube	0.305			
	0.487			
	0.715			
	0.995			
	1.305			
Square tube	0.282	0.279	0.284	1.02
	0.570	0.582	0.558	0.959
	0.955	0.956	0.953	0.997
High aspect ratio rectangular channel	0.225	0.116	4.00	34.5
	0.592	0.309	7.00	22.7
	0.957	0.504	10.0	19.8

then becomes nearly constant. As shown in Fig. 2, liquid film thickness just after the initial decreasing period is defined as initial liquid film thickness δ_0 .

In the present study, water, ethanol and FC-40 were used as working fluids. For the gas phase, air was always used throughout this study. All experiments were conducted under room temperature and atmospheric pressure. Viscosity and density of the liquid phase are used for calculating Reynolds and capillary numbers. For a given capillary number, Reynolds number of water is nearly 5 times larger than that of ethanol, and about 30 times larger than that of FC-40. By using different diameter tubes and working fluids, it is possible to cover wide ranges of Reynolds and capillary numbers.

3. EXPERIMENTAL RESULTS

3.1 Steady circular tube flow

Figure 3 shows initial liquid film thicknesses normalized by tube diameter against capillary number, $Ca = \mu U / \sigma$, in steady circular tubes. Open symbols are the measured data for water, ethanol and FC-40, respectively. It is clearly seen that the inertial force has a strong effect on liquid film thickness even in the laminar flow range of $Re < 2000$. The solid lines are the

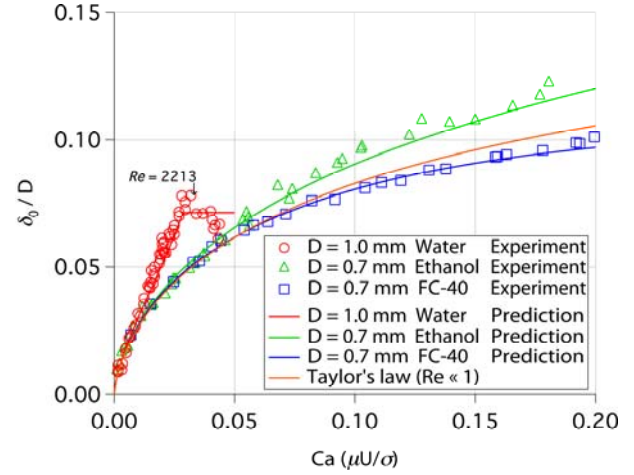


Figure 3 Predicted initial liquid film thickness δ_0 .

predicted liquid thicknesses using following correlation, which was obtained from a scaling analysis.

$$\left(\frac{\delta_0}{D_h} \right)_{\text{steady}} = \frac{0.670 Ca^{\frac{2}{3}}}{1 + 3.13 Ca^{\frac{2}{3}} + 0.504 Ca^{0.672} Re^{0.589} - 0.352 We^{0.629}} \quad (Ca < 0.3, Re < 2000), \quad (1)$$

where $Ca = \mu U / \sigma$ and $Re = \rho U D h / \mu$ and $We = \rho U^2 D h / \sigma$. As shown in Fig. 3, the present correlation can predict liquid film thickness very accurately.

3.2 Steady square tube flow

Dimensionless bubble radii R_{center} and R_{corner} are the common parameters used in square channels:

$$R_{\text{center}} = 1 - \frac{2\delta_{0,\text{center}}}{D_h}, \quad (2)$$

$$R_{\text{corner}} = \sqrt{2} - \frac{2\delta_{0,\text{corner}}}{D_h}. \quad (3)$$

The experimental correlations for R_{center} and R_{corner} are obtained by optimizing the coefficients and exponent values with the least linear square method as follows:

$$R_{\text{corner}} = 1.171 - \frac{2.43 Ca^{\frac{2}{3}}}{1 + 7.28 Ca^{\frac{2}{3}} - 0.255 We^{0.215}}, \quad (4)$$

$$R_{\text{center}} \cong \begin{cases} 1 & (R_{\text{corner}} > 1) \\ R_{\text{corner}} & (R_{\text{corner}} \leq 1) \end{cases}. \quad (5)$$

Figure 4 shows the comparison between the experimental data and the predicted results. Liquid film thickness becomes thicker, i.e. R gets smaller, as Reynolds number increases. Present correlation can predict dimensionless bubble diameters within the range of $\pm 5\%$ accuracy.

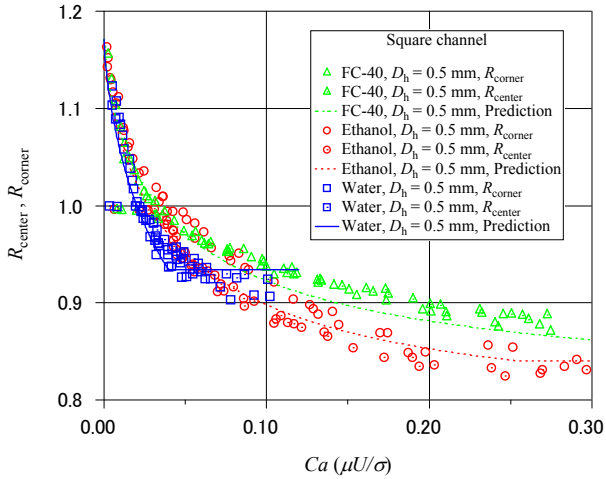


Figure 4 Predicted bubble diameter in $D_h = 0.5$ mm square tube.

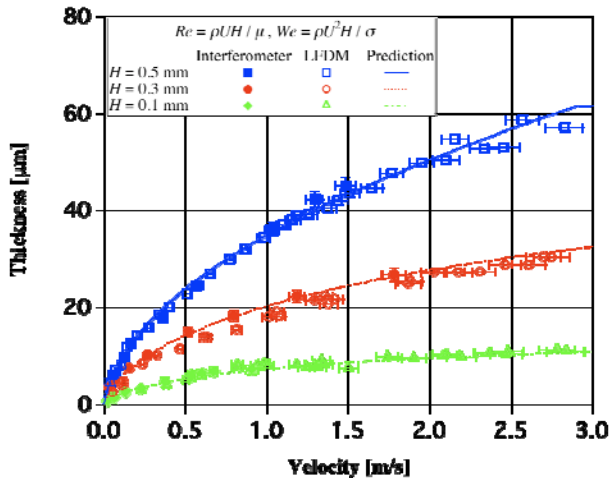


Figure 5. Comparison between measured and predicted initial liquid film thicknesses in high aspect ratio rectangular channels.

3.3 High aspect ratio rectangular channels

For high aspect ratio rectangular channels, interferometer as well as laser confocal displacement meter are used to measure liquid film thickness. Figure 5 shows measured initial liquid film thicknesses by interferometer and laser confocal displacement meter. Both results are in very good agreement, which proves the reliability of both methods for liquid film thickness measurement.

From the analogy between flows in circular tubes and parallel plates, it is demonstrated that dimensionless expression of liquid film thickness in parallel plates takes the same form as that of the circular tube, if D_h is replaced by channel height H . In Fig. 5, prediction is also shown using Eq. (1) with hydraulic diameter as the characteristic length for Reynolds and Weber numbers. Circular tube correlation can predict initial liquid film thickness in high aspect ratio rectangular channel remarkably well.

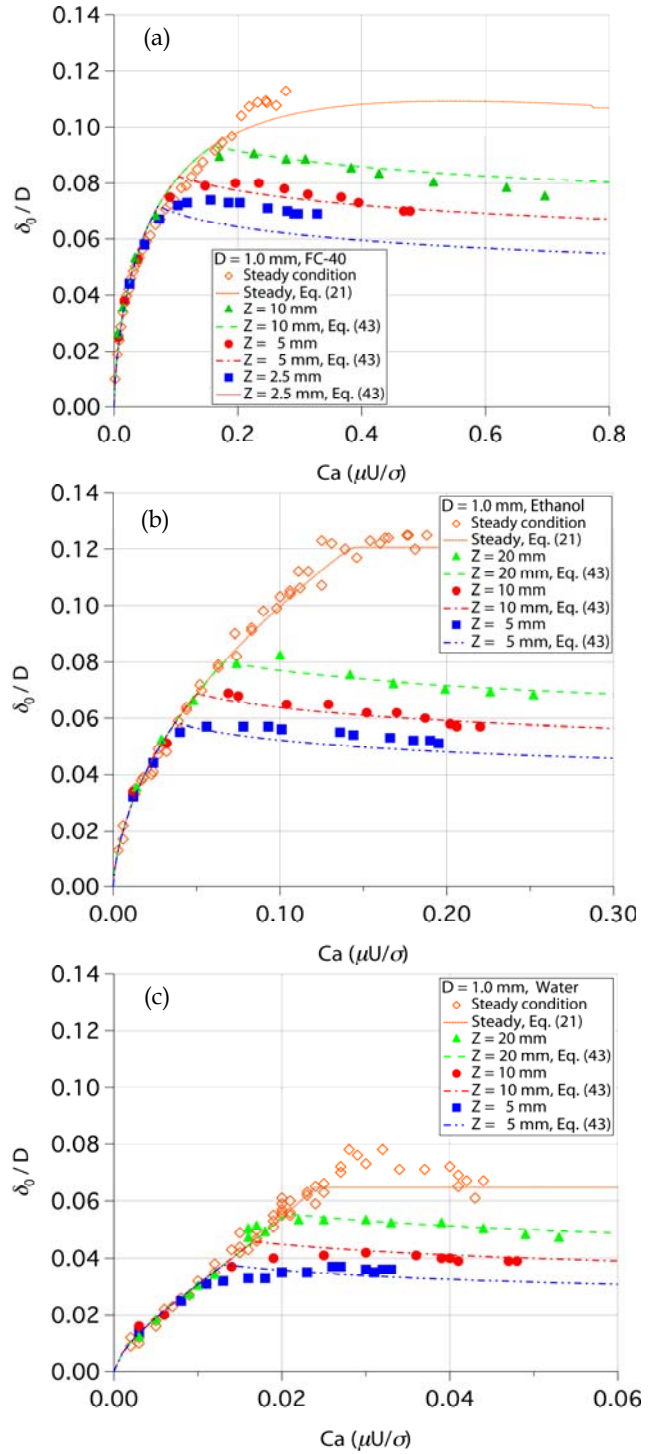


Figure 6 Initial liquid film thicknesses in accelerated circular tubes. (a) FC-40, (b) ethanol and (c) water.

3.4 Accelerated circular tube flow

In order to investigate the flow acceleration effect on the liquid film thickness, measurement points are positioned at $Z = 5, 10$ and 20 mm away from the initial air-liquid interface position ($Z = 0$ mm). The bubble position is measured from the image captured by the high-speed camera.

Figure 6 (a)-(c) show the dimensionless initial liquid film thicknesses in $D_h = 1.0$ mm circular tube for FC-40, ethanol and water, respectively. As shown in the figure, initial liquid film thickness under accelerated condition can be divided into two regions. At small capillary numbers, initial liquid film thickness is identical to the steady case. As capillary number increases, initial liquid film thickness deviates from the steady case and becomes much thinner.

Under accelerated conditions, Bond number based on bubble acceleration a is introduced as follows:

$$Bo = \frac{\rho a D^2}{\sigma} \quad (6)$$

The initial liquid film thickness correlation under flow acceleration is obtained using Bond number as:

$$\left(\frac{\delta_0}{D_h} \right)_{\text{acceleration}} = \frac{0.968 Ca^{\frac{2}{3}} \cdot Bo^{-0.414}}{1 + 4.838 Ca^{\frac{2}{3}} \cdot Bo^{-0.414}} \quad (7)$$

As shown in Fig. 6, initial liquid film thickness in steady and accelerated flows are identical when capillary number is small. Thus, in the present study, initial liquid film thickness in the whole capillary number range is simply expressed by combining steady and accelerated correlations as follows:

$$\frac{\delta_0}{D_h} = \min \left[\left(\frac{\delta_0}{D_h} \right)_{\text{steady}}, \left(\frac{\delta_0}{D_h} \right)_{\text{acceleration}} \right], \quad (8)$$

where, Eq. (1) is used for $(\delta_0/D_h)_{\text{steady}}$ and Eq. (7) is used for $(\delta_0/D_h)_{\text{acceleration}}$. The predicted liquid film thicknesses by Eq. (8) are plotted together with the experimental data in Fig. 6. As can be seen from the figure, Eq. (8) can predict initial liquid film thickness under acceleration very well for three different working fluids.

4. CONCLUSIONS

The liquid film thickness in a micro tube is measured by laser confocal displacement meter. The effect of inertial force can not be neglected even in the laminar liquid flow regime. From the scaling analysis, empirical correlation for the dimensionless initial liquid film thickness based on capillary number, Reynolds number and Weber number is proposed. In square tubes, liquid film formed at the center of the side wall becomes very thin at small capillary numbers. However, as capillary number increases, the bubble shape becomes nearly axisymmetric. As Reynolds number increases, flow transits from non-axisymmetric to axisymmetric at

smaller capillary numbers. Initial liquid film thickness in high aspect ratio rectangular channels can be predicted well using the circular tube correlation provided that hydraulic diameter is used for Reynolds and Weber numbers. It is also shown that results from interferometer and laser confocal displacement meter give nearly identical results, which proves the reliability of both methods.

When the flow is accelerated, liquid film becomes much thinner than the steady case. In order to develop precise micro-scale two-phase heat transfer models, it is necessary to consider the effect of flow acceleration on the liquid film formation.

5. ACKNOWLEDGEMENT

The authors would like to thank Prof. Kasagi, Prof. Suzuki and Dr. Hasegawa for the fruitful discussions and suggestions. This work is supported through Grant in Aid for Scientific Research (No. 20560179) and Global COE program, Mechanical Systems Innovation, by MEXT, Japan.

6. REFERENCES

- [1] Niiyama, Y., Yatsuzuka, S., Fukuda, K., Hagiwara, Y., Nishizawa, K. and Shikazono, N., *Proc. ICOPE-II*, POWER2011-55394 (2011).
- [2] Ding, Y., Bi, H. T. & Wilkinson, D. P., *J. Power Sources*, 196, 6282-6292 (2011).
- [3] Thome, J. R., Dupont, V. & Jacobi, A. M., *Int. J. Heat Mass Transf.*, 47, 3375-3385 (2004).
- [4] Taylor, G. I., *J. Fluid Mech.*, 10, 161-165 (1961).
- [5] Aussillous, P. & Quere, D., *Physics of Fluids*, 12, 2367-2371 (2000).
- [6] Kreutzer, M. T., Kapteijn, F., Moulijn, J. A., Kleijn, C. R. & Heiszwolf, J. J., *AIChE J.*, 51(9), 2428-2440 (2005).
- [7] Tibirica, C. B., Nascimento, F. J. & Ribatski, G., *Exp. Therm. Fluid Sci.*, 34 (4), 463-473 (2010).
- [8] Han, Y. & Shikazono, N., *Int. J. Heat Fluid Flow*, 30(5), 842-853 (2009).
- [9] Han, Y. & Shikazono, N., *Int. J. Multiphase Flow*, 35(10), 896-903 (2009).
- [10] Han, Y. & Shikazono, N., *Int. J. Heat Fluid Flow*, 31(4), 630-639 (2010).
- [11] Han, Y.; Shikazono, N. & Kasagi, N., *Int. J. Multiphase Flow*, 37(1), 36-45 (2009).
- [12] Shikazono, N. & Han, Y., *Heat Transfer*, InTech, in press (2011).
- [13] Han, Y., Shikazono, N. and Kasagi, N., *Proc. 8th ASME-JSME Therm. Eng. Joint Conf.*, AJTEC2011-44190 (2011).